Superconducting- and normal-state thermal conductivity of $NbSe_2$

F. Roeske, Jr.,* H. R. Shanks, and D. K. Finnemore
Ames Laboratory—ERDA and Department of Physics, Iowa State University, Ames, Iowa 50011
(Received 16 May 1977)

Thermal-conductivity measurements have been used to study the temperature dependence of the scattering of phonons and electrons in single crystals of the superconducting layer compound $NbSe_2$ between 1 and 10 K. In this temperature range, the results agree with standard theoretical models for a three-dimensional metal. The magnetoresistance has a very strong linear magnetic-field dependence as might be expected if there were magnetic breakdown at superzone gaps induced by charge-density waves.

INTRODUCTION

Layer compounds such as $NbSe_2$ hold a special place in the study of superconductivity because they have highly anisotropic chemical bonding and because they show charge-density wave phenomena with the attendant lattice instabilities. Many of the superconducting properties of these quasi-two-dimensional metals have been studied previously and a fairly detailed picture has been developed to explain the electronic character. For example, Morris and Coleman[1] have measured the energy gap for electrons traveling perpendicular to the layers via electron tunneling, and they find a value much smaller than the Bardeen-Cooper-Schrieffer[2] theory (BCS) predicts. Clayman[1] has studied the orientation dependence of the gap via infrared absorption and has found a gap for electrons moving parallel to the layers close to the BCS prediction, whereas the gap for electrons moving perpendicular to the layers is much smaller. Hence, the tunneling and infrared data are consistent and show an anisotropy of about 70% Several groups have studied the anisotropy of both the electrical resistivity and the upper critical field[3] and have found pronounced angular dependences. In addition, Frindt[4] has measured the superconducting transition temperature T_c and finds that T_c is suppressed only about 20% as the thickness is reduced to a few angstroms by peeling off successive layers. Even though there are marked anisotropies in many transport properties, the thermodynamic properties are close to the predictions for an ordinary three-dimensional metal.

The normal-state properties of $NbSe_2$ show very clear evidence of charge-density-wave behavior as shown by the electron-diffraction work of Wilson *et al.*,[5] the neutron-scattering work of Moncton *et al.*,[6] and the specific-heat work of Harper *et al.*[7] One of the interesting aspects of $NbSe_2$ is that the occurrence of the charge-density wave (CDW) depends on the normal-state mean free path of the electrons. As shown by Huntley and Frindt,[8] long-mean-free-path samples show a CDW transition at 33.5 K and a Hall-coefficient reversal, but the samples with resistivities higher than 30 $\mu\Omega$ cm show neither the Hall-coefficient reversal nor the charge-density waves. A similar effect occurs when Fe and Mn are added in positions between the layers.[9]

We have undertaken a study of the thermal conductivity in $NbSe_2$ to determine whether there are special scattering processes associated with charge-density waves or with the quasi-two-dimensional character of bonding. In this system, phonons are a major carrier of heat, comparable to the electrons, so the separation of phonon-scattering mechanisms is easier than in many metals. The general approach is to measure both the electrical and thermal conductivity of the same sample over a wide range of temperature and magnetic field in both superconducting and normal state in order to unravel the various scattering mechanisms.

EXPERIMENTAL

Sample preparation

Single crystals of $NbSe_2$ were prepared by iodine vapor transport in a 5-cm-diam by 25-cm-long quartz tube. For sample 1, the reaction of the Nb and Se was carried out at 750 °C and the material was transported to 715 °C. For samples 2 and 3, the corresponding temperatures were 600 and 580 °C. After 14 days of transport, a number of single crystals up to $8 \times 8 \times 0.1$ mm were obtained at the cool end of the tube. Samples were cooled to room temperature slowly. These transported samples were then heated to 100 °C in a vacuum of 10^{-6} Torr for 48 h to remove the iodine. Mass spectrographic analysis showed that the major impurity in samples 2 and 3 was tantalum at 600 ppm. For sample 1, the major impurities were tantalum and iron at the 100 ppm level.

Measurements

Thermal-conductivity data with heat flow parallel to the layers were taken by a steady-state method with temperatures determined by two calibrated germanium thermometers, GR65 and GR99. These are very stable Honeywell thermometers which have been calibrated several times over a period of 15 years. The most recent calibration was done on GR65 by Anderson and Swenson from 1 to 77 K in 1974.[10] GR99 was calibrated in detail earlier[11] and it was compared with GR65 in these measurements. The magnetoresistance of these thermometers in 50 kOe is comparable to the total zero-field resistance so a rather careful calibration in field is required. To establish the temperature scale in a field, a capacitance thermometer sensitive to 0.1 mK was used to define a fixed temperature as the field increased. Measurements against the vapor pressure of ^{4}He at 4.2 K indicate the capacitance is independent of field. Difficulties of drift in capacitance with time were noted shortly after a temperature change, but the capacitance thermometer never took more than 30 min to stabilize to better than 1 mK. Considerable care was taken to retain the orientation of the thermometer relative to the applied magnetic field direction because the magnetoresistance is dependent on orientation.[12] The calibration was checked each run to determine whether this orientation had shifted.

The most serious experimental problem in these measurements is the attachment of heater and thermometer contacts to give uniform heat flow and a well defined length to area ratio. The samples are small, fragile, and anisotropic so considerable care is required in attaching both thermal and electrical leads. Copper strips, which were used to thermally connect the thermometer to the sample were wrapped around the sample and affixed to all four sides with GE7031 varnish. Electrical leads were attached with DuPont 4018 silver paint. In an attempt to give uniform heat flow, the heater was attached across the end of the sample so that all of the layers were in contact with both the source and sink for heat. This sample assembly is shown in Fig. 1. For these samples, the size of the copper strip leading to the thermometer is comparable to the distance between leads so there is a substantial uncertainty in the length to area (l/A) measurement. The error in l/A might be as large as a factor of 2 because the thermometer temperature cannot be identified with a well-defined position on the sample. The precision of the measurement is about 1% but the absolute value of the conductivity is not well measured in this experiment.

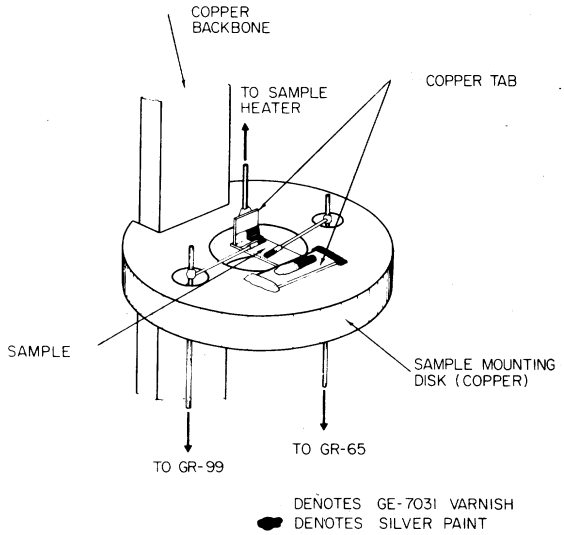

FIG. 1. Sample holder geometry.

RESULTS AND DISCUSSION

The thermal conductivity of these $NbSe_2$ samples parallel to the lamina is rather low compared to most pure metals and indeed is comparable to ordinary brass. As shown in Fig. 2, the conductivity at 8 K is about 70 mW/cm K. At first sight the general shape of the normal state data is similar for all three samples but there is a marked difference in the shape of the superconducting state data. For sample 1 of Fig. 2(a), there is a sharp change in slope at the superconducting transition as would be expected if the electrons are the dominant carrier of heat. For sample 2 of Fig. 2(b), there is only a minor change in slope at T_c as would be expected if the phonon conductivity were comparable to the electronic conductivity. Sample 3 is similar to sample 2 so it is not shown. Sample 1 differs from samples 2 and 3 primarily because the mean free path for electrons is much longer.

Thermal conductivity data by themselves are difficult to analyze because there are at least two carriers of heat, the electrons and phonons, and there are a number of different scattering mechanisms for each carrier. Hence, thermal conductivity data as a function of temperature are usually not sufficient. Fortunately, electrons carry both electric charge and heat, whereas phonons carry only heat so the electrical conductivity is helpful additional data. In addition, the mean free path of electrons depends strongly on magnetic field, whereas the phonon mean free path is nearly independent of magnetic field, so the magnetoresistance is helpful in separating terms. Hence, we have measured both the electrical and thermal conductivity over a range of temperatures and magnetic fields to permit an analysis of the various contributions.[13,14]

Magnetoresistance

An applied field perpendicular to the lamina ($\vec{H} \| \vec{c}$) has a very strong effect on the thermal resistivities as

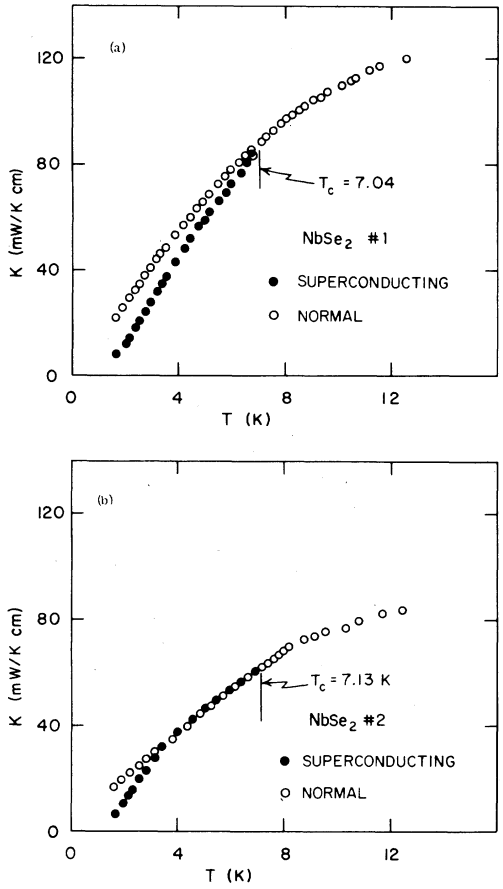

FIG. 2. Thermal conductivity of $NbSe_2$ in the superconducting (solid circles) and normal states (open circles). Below T_c, the normal-state data are corrected for magnetoresistance as described in the text.

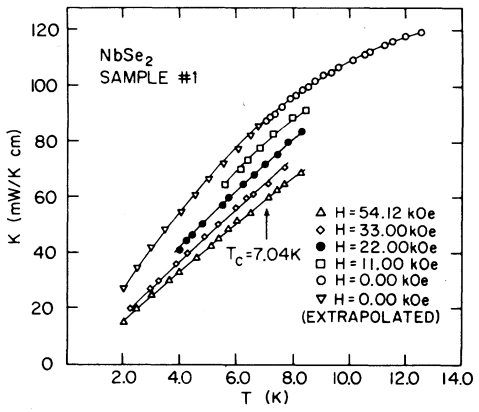

FIG. 3. Magnetic field dependence of the normal-state thermal conductivity of $NbSe_2$.

exemplified by the thermal magnetoresistance of Fig. 3. For sample 1, an applied field of 54 kOe reduces the conductivity at 8 K by about $\frac{1}{3}$. For samples 2 and 3, the effect is somewhat smaller because the electrons carry a smaller fraction of the heat for these samples. To see the magnetic field dependence more quantitatively, the change in thermal resistance (ΔW) and the electrical resistance ($\Delta\rho$) as a function of magnetic field are plotted on Figs. 4(a) and 4(b). For sample 2, the electrical resistivity rises by about 1%/kOe, whereas the thermal resistance rises about 0.4%/kOe. Presumably the phonon carriers are unaffected by the magnetic field so the factor of two difference in slope of the magnetoresistance indicates that at this temperature the phonons and electrons carry about $\frac{1}{3}$ and $\frac{2}{3}$ of the heat, respectively.

The linear character of both the thermal and electrical magnetoresistance is a point of central interest in this work because it is further evidence of charge density waves in these layer compounds. As pointed out

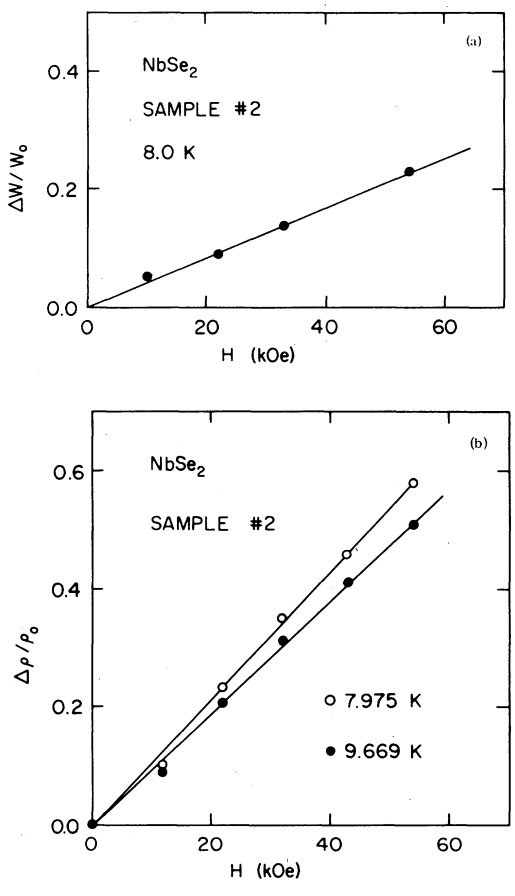

FIG. 4. Magnetoresistance of $NbSe_2$ sample 2. The electrical resistance decreases about 1%/kOe whereas the thermal resistance decreases about 0.4%/kOe.

by Overhauser,[15] the existence of charge density wave superzone energy gaps provides a scattering mechanism which would give a linear magnetoresistance. In this model, the scattering frequency is controlled by the frequency with which electrons encounter the energy gap, the cyclotron frequency, so the probability of scattering is linear in magnetic field. There are, of course, other models which could give a linear magnetoresistance so it is not certain that the charge density waves are solely responsible for the effect, but the data are certainly suggestive.

The traditional way of presenting thermal conductivity data for superconductors is to compute the ratio of the superconducting to normal state conductivities K^S/K^N and compare this ratio with the predictions of theory. In most metals the upper critical field H_{c2} is less than 1 or 2 kOe and the magnetoresistance does not change the conductivity significantly for a field change this small. For these layer compounds, however, the situation is quite different. Upper critical fields can be on the order of hundreds of kOe,[2] and the thermal conductivities can change by factors of 2 in this range. Therefore, to present the data in the traditional form it is necessary to extrapolate the normal state conductivity to the value it would have had in the normal state with no magnetoresistance.

At present, there is no adequate theory for the magnetoresistance of these quasi-two-dimensional compounds so a semiempirical extrapolation procedure based on the Sondheimer-Wilson two-band model has been used.[16] The data are fit to an equation of the form

$$\Delta W/W(0) = CH^m T^{-n}/(1 + DH^m T^{-n}) \ ,$$

where $W(0)$ is the resistance in zero field and C, D, m, and n are constants. If the $m = n = 2$ then the formula would be the Sondheimer-Wilson model. In the temperature range above T_c where the full magnetic field range is available the exponent for the magnetic field and temperature can be determined and the data give $m \approx 1.3$ and $n \approx 1.6$ for sample 2. The magnetic field coefficient m is nearly the same within 10% for all samples, but the temperature coefficient n varies by 50% from sample to sample. For our purposes here, the fact that the coefficient m is the same for all samples means that the thermal conductivity can be extrapolated to zero field with some confidence. These extrapolated values are shown as the open triangles of Fig. 3.

Superconducting-state data

The ratio of the total thermal conductivity in the superconducting state K_T^S to that in the normal state K_T^N is shown in Fig. 5. On the figure it is clear that K_T^S/K_T^N for sample 1 drops away rather abruptly and falls monotonically toward zero. For sample 2 (solid

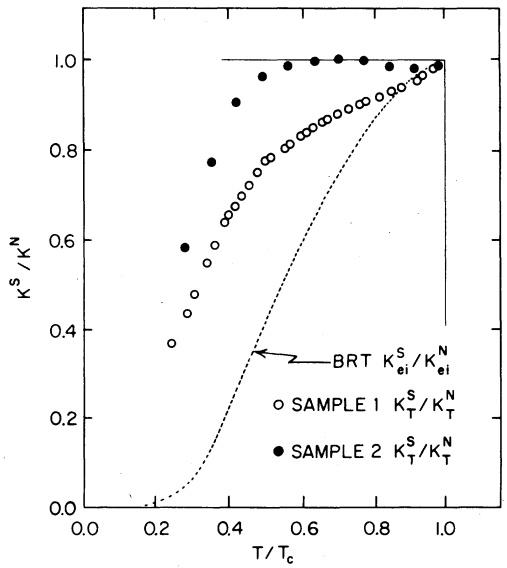

FIG. 5. Ratio of the total thermal conductivity in the superconducting state to that in the normal state. The dashed line represents the BRT prediction if the electrons were the only carrier and impurities the dominant scattering mechanism. Sample 2 differs from sample 1 primarily because the phonons carry a larger fraction of the total heat.

circles) K^S/K^N falls below 1, a small amount, at a reduced temperature of about 0.8 rises again and does not fall substantially below 1 until the reduced temperature T/T_c is less than 0.5. The rise in K^S/K^N, at a reduced temperature of about 0.7 occurs because the phonon conductivity is increasing markedly. As T/T_c decreases, the scattering of phonon by electrons decreases as the fraction of electrons in the superconducting ground state increase. The rise in K^S/K^N in this temperature range is common for samples in which the electrons are a major scatterer of phonons. The Bardeen, Rickayzen, and Tewordt[17] (BRT) calculation for the conductivity if electrons were the only carrier and the scattering is limited by impurity scattering (K_{ei}^S/K_{ei}^N) is shown for comparison. In this discussion, the superscript indicates whether the sample is superconducting or normal, the first subscript indicates the carrier and the second subscript indicates the scattering mechanism.

The thermal conductivity of a different layer compound, $TaSe_{0.4}S_{1.6}$, has been measured by Sichel, Serin, and Revelli[18] with results which are similar to $NbSe_2$ in some ways and different in others. They find that the superconducting state data lie only a few percent (always less than 10%) below the normal data so in this respect their data are similar to $NbSe_2$ samples 2 and 3 reported here. The tantalum chalcogenide results, however, differ from the data report-

ed here in that they find a positive curvature for the normal-state conductivity, whereas the $NbSe_2$ data show a negative curvature on a conductivity versus temperature plot. The $K^N \propto T^{1.6}$ law found for $TaSe_{0.4}S_{1.6}$ is quite different from the $NbSe_2$ data reported here.

Lorentz number

The electron and phonon contributions to the total thermal conductivity have been separated using the method developed by Gruneisen and Adenstedt[13] and de Haas and de Nobel.[14] In this method, it is assumed that the phonon conductivity K_g, and the Lorentz number L are independent of magnetic field so the conductivity can be written

$$K(H,T) = K_e(H,T) + K_g(T)$$

or

$$K(H,T) = L(T)\,T/\rho(H,T) + K_g(T) \quad . \tag{1}$$

For a fixed temperature a plot of $K(H)$ vs $T/\rho(H)$ has slope $L(T)$ and intercept $K_g(T)$.

The data lies on a straight line as expected and gives the Lorentz numbers shown on Fig. 6. Values of L are approximately 2×10^{-8} Ω W/K^2 at 7 K and rise to the free-electron value of 2.45×10^{-8} Ω W/K^2. The good fit to Eq. (1) and regular values of $L(T)$ tend to verify the basic assumptions of the separation into electron and phonon carrier contribution.

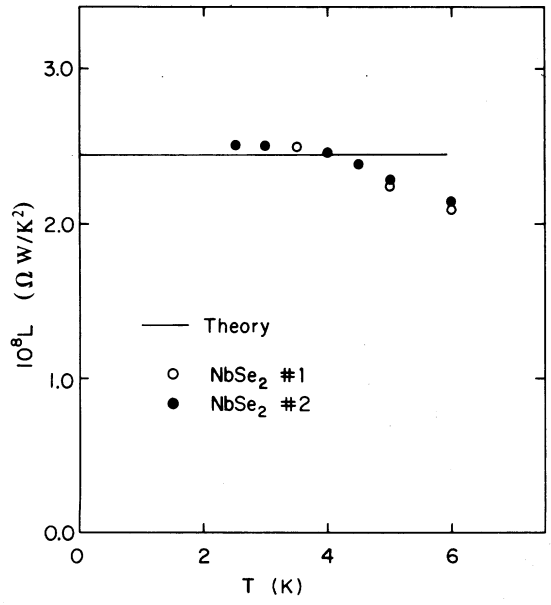

FIG. 6. Temperature dependence of the Lorentz number for samples 1 and 2.

Electronic conductivity

The primary scattering mechanisms for electron carriers are impurity scattering (K_{ei}^N) and phonon scattering (K_{eg}^N). Fitting the normal state electronic resistivity data to

$$W_e^N = (K_e^N)^{-1} = (K_{eg}^N)^{-1} + (K_{ei})^{-1} = AT^2 + B/T$$

or

$$W_e^N T = AT^3 + B \quad ,$$

one finds a rather good fit as shown in Fig. 7. The intercept then is determined by the impurity scattering and the slope is determined by the phonon scattering. The zero on the ordinate of Fig. 7 has been suppressed to show more detail of the data so it is clear that impurity scattering is dominant for these samples.

One can get a rough idea of the mean free path l associated with these scattering mechanisms from the kinetic theory expression for conductivity $K = \frac{1}{3}Cvl$, where C is the specific heat associated with the carrier and v is the velocity of the carrier. Using an electronic effective mass of 78% of the free mass, a Fermi velocity[19] of 0.51×10^8 cm/s, and a specific heat[20] γ of 10 mJ/mol K^2, one finds an impurity scattering mean free path of 150 Å for sample 2. A similar calculation for phonon scattering of electrons gives a mean free path of 1430 Å at 4 K for sample 2. Hence, at 4 K, electrons scatter from impurities at about 10 times the rate they scatter from phonons.

Phonon conductivity

A determination of the total phonon conductivity from Eq. (1) can be done by a simple subtraction and the results show that the phonons carry about $\frac{1}{3}$ of the total heat in the 4–10 K temperature range.

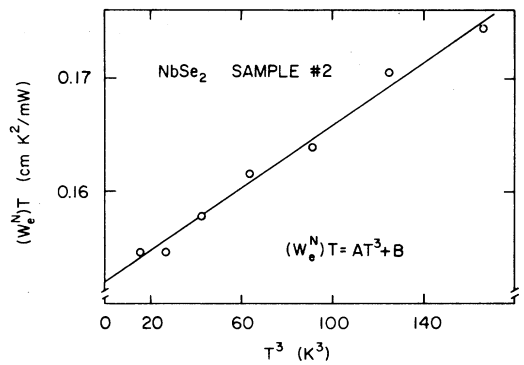

FIG. 7. A fit of electron thermal resistance W_e^N to phonon (AT^2) plus point defect (B/T) scattering. Point-defect scattering dominates.

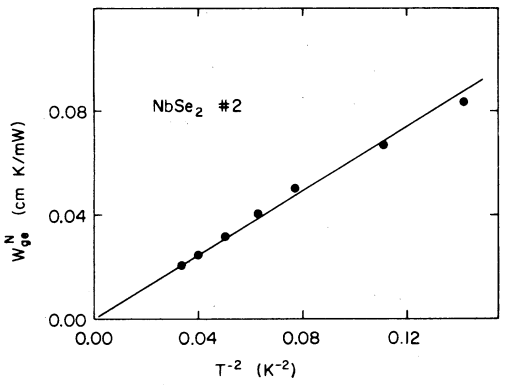

FIG. 8. Temperature dependence of the scattering of phonons by electrons. The magnitude of the resistance is somewhat lower than would be predicted for a spherical Fermi surface.

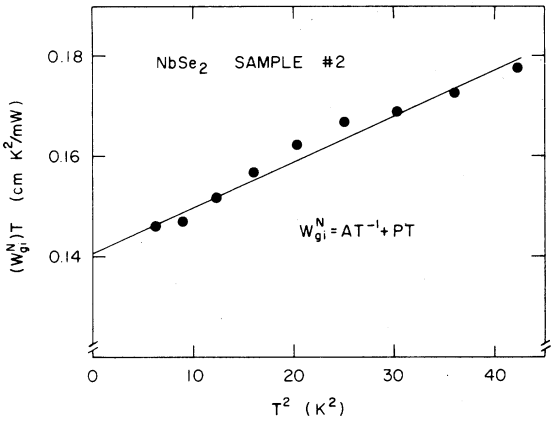

FIG. 9. Plot of the phonon thermal resistivity due to defects times the temperature T vs T^2.

Analysis of the scattering mechanisms for phonons, however, is complicated because there are many processes which are operative and different scattering processes have different temperature dependences. Both electron scattering and dislocation scattering of phonons give resistivities which vary as T^{-2} in the normal state,[21] ($W_{ge}^N + W_{gd}^N = AT^{-2}$), but electron scattering is smaller in the superconducting phase because the electrons condense into Cooper pairs.[17] The phonon resistivity due to point defects[22] goes linearly with T ($W_{ep}^N = K_{ep}^S = BT$). In addition, there may be a stacking fault term[23] which goes as CT^{-1}. At first sight there are so many variables that separation of the terms appears difficult. For completeness, however, we have taken an optimistic approach and have attempted the most reasonable separation. To do this, we have assumed (i) K_{ei}^S/K_{ei}^N is given by BRT with $\Delta = 1.76 k_B T_c$; (ii) $K_{ge}^S/K_{ge}^N = R(T)$ given by BRT; (iii) K_{eg}^S/K_{eg}^N is given by Tewordt; (iv) Impurity scattering of phonons is the same in the superconducting and normal state $K_{gi}^S = K_{gi}^N$. Assumption (i) may be questionable in view of the tunneling data,[1] but the carriers effective in transporting heat are the ones parallel to the layers and hence have the BCS gap.

With these assumptions, one can calculate the phonon resistivity due to electrons shown in Fig. 8. Full details of the point-by-point calculation of K_{gi} and K_{ge} are given elsewhere.[24] The resistivity has a T^{-2} temperature dependence and hence for the long wavelength phonons $NbSe_2$ behaves like a three-dimensional crystal. Values of the phonon mean free path are about a factor-of-2 longer than predicted from the Pippard model for the electron-phonon interaction for a metal with a spherical Fermi surface.[25] Hence, these K_{ge}^N results are entirely reasonable.

The phonon resistivity due to other defects,[22] W_{gi}^N, fits an equation of the form $W_{gi}^N = bT^{-1} + cT$ as shown in the plot of $W_{gi}^N T$ vs T^2 of Fig. 9. The rather small cT term (note suppressed zero on ordinate) can be associated with point defect scattering. The bT^{-1} term dominates the phonon scattering in this wavelength range and it has the temperature dependence which Klemens[23] predicts for stacking faults. If one assumes a Grueneisen parameter of 2, then the data would predict stacking fault for every 30 $NbSe_2$ layers for the $NbSe_2$ sample 2. In view of the weak Van der Waals bonding between layers, this result is not surprising.

SUMMARY

The thermal conductivity of these $NbSe_2$ samples parallel to the lamina is comparable to the conductivity of a relatively dirty metal such as brass. In the normal state, the magnetoresistance is very large and has a linear magnetic field dependence as would be expected if the scattering arose from magnetic breakdown at the superzone gaps caused by charge density waves. For the long-wavelength phonons typical of the 4–10 K temperature range, these laminar crystals behave in the same way as a normal three-dimensional metal.

ACKNOWLEDGMENTS

This work was supported by the U. S. ERDA Division of Physical Research. We would like to thank M. P. Zaitlin for discussions of various aspects of this work.

*Present address: University of California, Lawrence Livermore Laboratory L-45, Livermore, Calif. 94550.

[1]R. C. Morris and R. V. Coleman, Phys. Lett 43 A, 11 (1973); B. P. Clayman and R. F. Frindt, Solid State Commun. 9, 1881 (1971); B. P. Clayman, Can. J. Phys. 50, 3193 (1972).

[2]J. Bardeen, L. N. Cooper, and J. R. Schrieffer, Phys. Rev. 108, 1175 (1957).

[3]R. C. Morris, R. V. Coleman, and B. Bhandari, Phys. Rev. B 5, 895 (1972); R. C. Morris and R. V. Coleman, *ibid.* 7, 991 (1973); N. Toyota, H. Makatsuji, K. Noto, A. Hoshi, N. Kobayashi, Y. Muto, and Y. Onodera, J. Low Temp. Phys. 25, 485 (1976).

[4]R. F. Frindt, Phys. Rev. Lett. 28, 299 (1972).

[5]J. A. Wilson, F. J. Di Salvo, and S. Mahajan, Phys. Rev. Lett. 32, 882 (1974).

[6]D. E. Moncton, J. D. Axe, and F. J. Di Salvo, Phys. Rev. Lett. 34, 734 (1975).

[7]J. M. E. Harper, T. H. Geballe, and F. J. Di Salvo, Phys. Lett. 54 A, 27 (1975); A. J. Bevolo and H. R. Shanks, J. Appl. Phys. 45, 4644 (1974); K. E. Schwall, G. R. Stewart, and T. H. Geballe, J. Low Temp. Phys. 22, 557 (1976).

[8]D. J. Huntley and R. F. Frindt, Can. J. Phys. 52, 861 (1974).

[9]R. C. Morris, Phys. Rev. Lett. 34, 1164 (1975); D. J. Huntley, Phys. Rev. Lett. 36, 490 (1976).

[10]J. S. Rogers, R. J. Tainsh, M. S. Anderson, and C. A. Swenson, Metrologia 4, 47 (1968).

[11]D. K. Finnemore, T. F. Stromberg, and C. A. Swenson, Phys. Rev. 149, 231 (1966).

[12]L. J. Neuringer, A. J. Perlman, L. G. Rubin, and Y. Shapira, Rev. Sci. Instrum. 42, 9 (1971).

[13]E. Gruneisen and H. Adenstedt, Ann. Phys. (Leipz.) 31, 714 (1938).

[14]W. J. de Haas and J. de Nobel, Physica (Utr.) 5, 449 (1938).

[15]A. W. Overhauser, Phys. Rev. B 3, 3179 (1971); J. R. Reitz and A. W. Overhauser, Phys. Rev. 171, 749 (1968).

[16]E. H. Sondheimer and A. H. Wilson, Proc. R. Soc. Lond. 190, 435 (1947).

[17]J. Bardeen, G. Rickayzen, and L. Tewordt, Phys. Rev. 113, 982 (1959).

[18]E. K. Sichel, B. Serin, and J. F. Revelli, J. Low Temp. Phys. 16, 229 (1974).

[19]J. E. Graebner and M. Robbins, Phys. Rev. Lett. 36, 422 (1976).

[20]A. J. Bevolo and H. R. Shanks, J. Appl. Phys. 45, 4644 (1974).

[21]J. M. Ziman, Nuovo Cimento Suppl. 7, 353 (1958).

[22]J. M. Ziman, *Electrons and Phonons* (Clarendon, Oxford, 1960).

[23]P. G. Klemens, Can. J. Phys. 35, 441 (1957); W. R. G. Kemp, P. G. Klemens, and R. J. Tainsh, Philos. Mag. 4, 815 (1959).

[24]F. Roeske, Jr., Ph.D. thesis (Iowa State University, 1976) (unpublished).

[25]A. B. Pippard, J. Phys. Chem. Solids 3, 175 (1957); P. Lindenfeld and W. B. Pennebaker, Phys. Rev. 127, 1881 (1962).